Supporting Information

Ambient Ionization and FAIMS Mass Spectrometry for Enhanced Imaging of Multiply Charged Molecular Ions in Biological Tissues

Clara L. Feider[1], Natalia Elizondo[1], and Livia S. Eberlin[1]*

[1] Department of Chemistry, The University of Texas at Austin, Austin, TX, 78712

** to whom correspondence may be addressed: liviase@utexas.edu*

Table of Contents

Supporting Table 8. MS/MS fragments for human hemoglobin α-subunit.

Supporting Figure 13. LMJ-SSP and LMJ-SSP-FAIMS-MS protein ion image replicates.

Supporting Figure 14. LMJ-SSP-FAIMS-MS ion images of lipids and proteins of an unwashed rat brain tissue section.

Supporting Figure 15. Voxel versions of ion images displayed in the main article using the interpolate function.

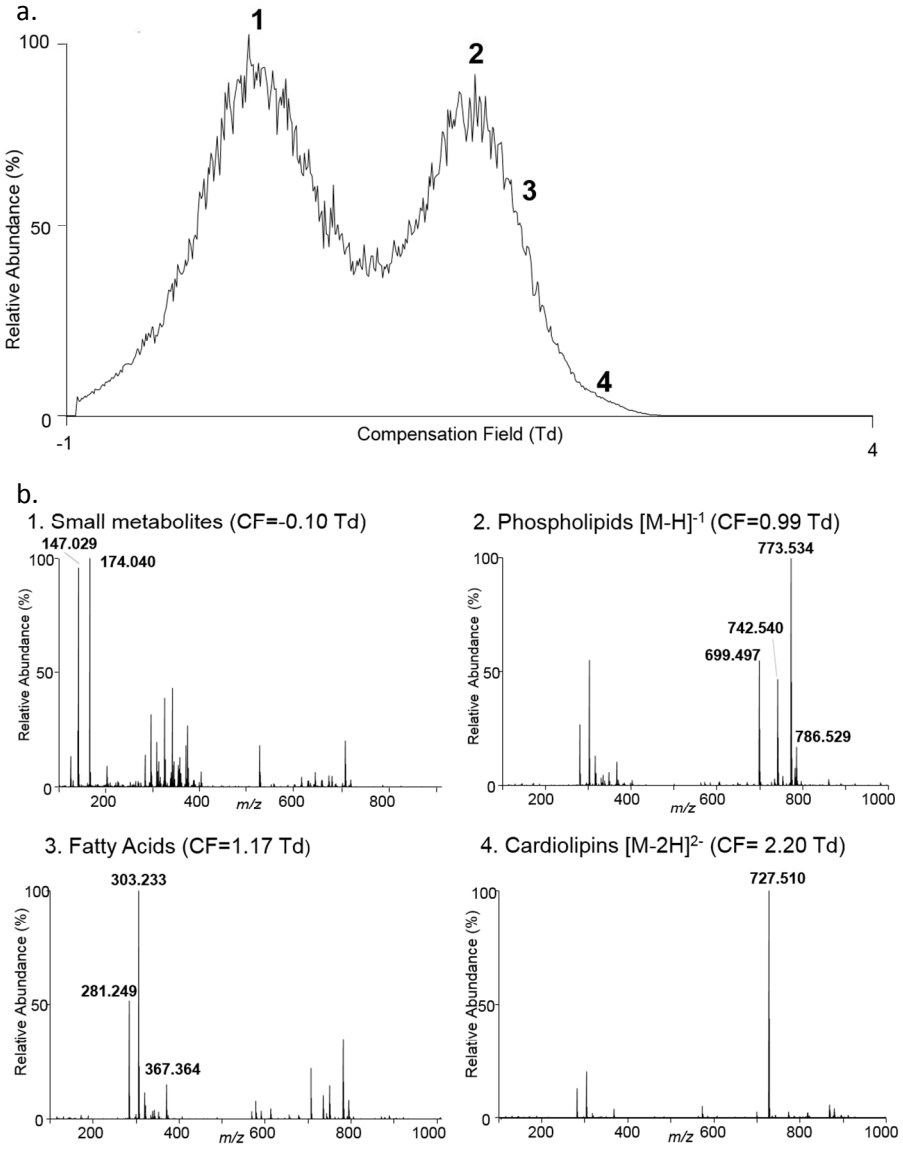

Figure S1. a) Chromatogram of a compensation field sweep (-1-4 Td) at a dispersion field of 220 Td, in which numbers annotating the peak field values for the transmission of different molecular classes of interest: metabolites, fatty acids, phospholipids, and doubly-charged

species, i.e. cardiolipin b) Spectra corresponding to the compensation field at which peak transmission of each molecular class.

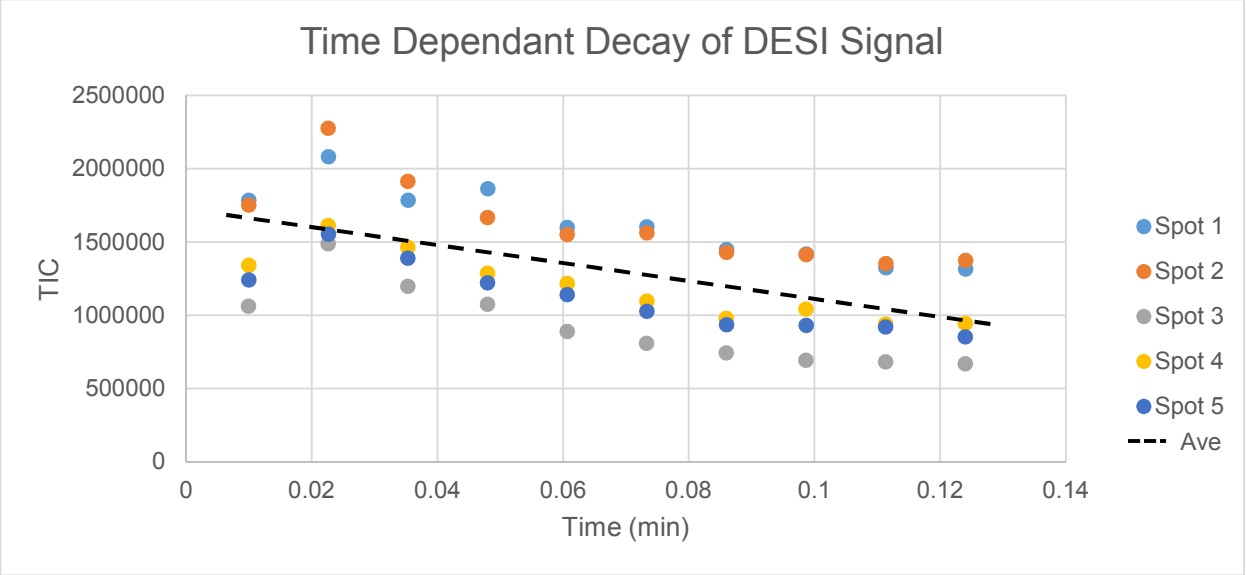

Figure S2. Time-dependent decay of DESI signal for analysis of five representative spots for 6 seconds (0.10 min) each, without FAIMS sweep, and an average trend line for the total loss in ion intensity throughout the scan.

Table S1. Representative CL species detected during DESI-MSI and FAIMS-DESI-MSI analysis of rat brain tissue.[a]

Measured *m/z*	Mass Error (ppm)[b]	Proposed Formula
697.4654	-3.15	$C_{77}H_{138}O_{17}P_2$
698.4718	-1.15	$C_{77}H_{140}O_{17}P_2$
699.4803	-2.14	$C_{77}H_{142}O_{17}P_2$
700.4885	-2.57	$C_{77}H_{144}O_{17}P_2$
709.4647	-2.11	$C_{79}H_{138}O_{17}P_2$
710.4727	-2.39	$C_{79}H_{140}O_{17}P_2$
711.4796	-1.12	$C_{79}H_{142}O_{17}P_2$
712.4876	-1.26	$C_{79}H_{144}O_{17}P_2$
713.4955	-1.40	$C_{79}H_{146}O_{17}P_2$
714.5012	1.54	$C_{79}H_{148}O_{17}P_2$
715.5065	5.59	$C_{79}H_{150}O_{17}P_2$
717.4803	-2.09	$C_{80}H_{142}O_{17}P_2$
718.489	-3.20	$C_{80}H_{144}O_{17}P_2$
719.4963	-2.50	$C_{80}H_{146}O_{17}P_2$
720.5048	-3.47	$C_{80}H_{148}O_{17}P_2$

721.4654	-3.05	$C_{81}H_{138}O_{17}P_2$
722.4727	-2.35	$C_{81}H_{140}O_{17}P_2$
723.4806	-2.49	$C_{81}H_{142}O_{17}P_2$
724.4878	-1.52	$C_{81}H_{144}O_{17}P_2$
725.4943	0.28	$C_{81}H_{146}O_{17}P_2$
726.5029	-0.83	$C_{81}H_{148}O_{17}P_2$
727.5103	-0.27	$C_{81}H_{150}O_{17}P_2$
728.516	2.75	$C_{81}H_{152}O_{17}P_2$
729.4827	-5.35	$C_{82}H_{142}O_{17}P_2$
729.5254	0.55	$C_{81}H_{154}O_{17}P_2$
730.4873	0.00	$C_{82}H_{144}O_{17}P_2$
731.4947	-0.27	$C_{82}H_{146}O_{17}P_2$
733.4658	-3.54	$C_{83}H_{138}O_{17}P_2$
734.4726	-2.18	$C_{83}H_{140}O_{17}P_2$
735.4803	-2.04	$C_{83}H_{142}O_{17}P_2$
736.4874	-0.95	$C_{83}H_{144}O_{17}P_2$
737.4956	-1.49	$C_{83}H_{146}O_{17}P_2$
738.5032	-1.22	$C_{83}H_{148}O_{17}P_2$
739.5087	1.89	$C_{83}H_{150}O_{17}P_2$
740.5154	3.51	$C_{83}H_{152}O_{17}P_2$
741.5216	0.00	$C_{83}H_{154}O_{17}P_2$
742.4877	-1.35	$C_{84}H_{144}O_{17}P_2$
746.4734	-3.22	$C_{85}H_{140}O_{17}P_2$
747.4812	-3.21	$C_{85}H_{142}O_{17}P_2$
748.4878	-1.47	$C_{85}H_{144}O_{17}P_2$
749.4952	-0.93	$C_{85}H_{146}O_{17}P_2$
750.502	0.40	$C_{85}H_{148}O_{17}P_2$
751.5093	1.06	$C_{85}H_{150}O_{17}P_2$
752.5164	2.13	$C_{85}H_{152}O_{17}P_2$
753.5249	1.19	$C_{85}H_{154}O_{17}P_2$
754.4879	0.00	$C_{86}H_{144}O_{17}P_2$
755.4946	-0.13	$C_{86}H_{146}O_{17}P_2$
758.4722	-1.58	$C_{87}H_{140}O_{17}P_2$
759.48	-1.58	$C_{87}H_{142}O_{17}P_2$
760.4874	-0.92	$C_{87}H_{144}O_{17}P_2$
761.4949	-0.53	$C_{87}H_{146}O_{17}P_2$
762.5031	-1.05	$C_{87}H_{148}O_{17}P_2$
763.5108	-0.92	$C_{87}H_{150}O_{17}P_2$
764.5217	-4.84	$C_{87}H_{152}O_{17}P_2$

765.5277	-2.48	$C_{87}H_{154}O_{17}P_2$
770.4733	-2.99	$C_{89}H_{140}O_{17}P_2$
771.4806	-2.33	$C_{89}H_{142}O_{17}P_2$
772.4886	-2.46	$C_{89}H_{144}O_{17}P_2$
773.495	-0.65	$C_{89}H_{146}O_{17}P_2$
774.5007	2.07	$C_{89}H_{148}O_{17}P_2$
775.5109	-1.03	$C_{89}H_{150}O_{17}P_2$
776.5178	0.26	$C_{89}H_{152}O_{17}P_2$
777.5264	-0.77	$C_{89}H_{154}O_{17}P_2$
783.4798	-1.28	$C_{91}H_{142}O_{17}P_2$
784.4882	-1.91	$C_{91}H_{144}O_{17}P_2$
785.4935	1.27	$C_{91}H_{146}O_{17}P_2$
786.4991	4.07	$C_{91}H_{148}O_{17}P_2$
795.4814	-3.27	$C_{93}H_{142}O_{17}P_2$
796.4873	-0.75	$C_{93}H_{144}O_{17}P_2$
797.4937	1.00	$C_{93}H_{146}O_{17}P_2$
798.4994	3.63	$C_{93}H_{148}O_{17}P_2$

[a] Red text denotes species that were only detectable with the addition of FAIMS with DESI-MSI

[b] Calculated based on the exact monoisotopic *m/z* of the deprotonated molecular ion.

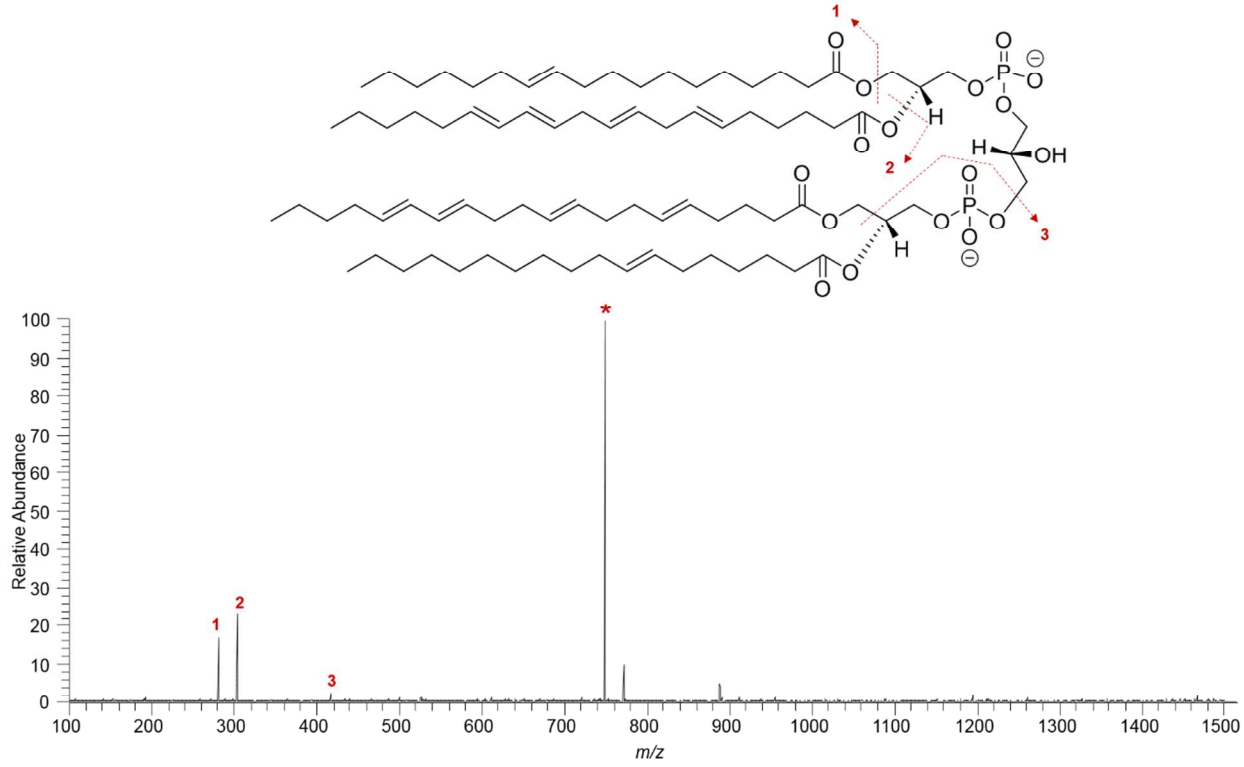

Figure S3. MSMS of *m/z* 749.495, identified at CL (20:4/20:4/20:4/18:1)

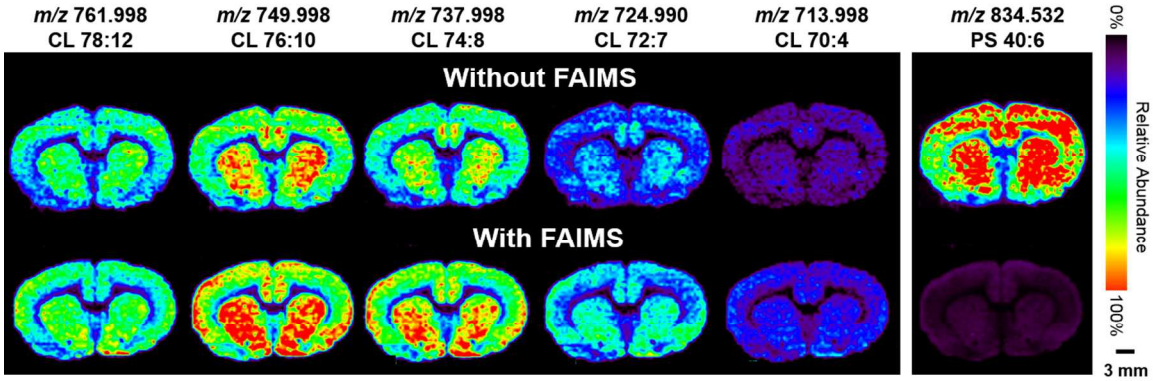

Figure S4. DESI-MS and DESI-FAIMS-MS ion images of rat brain tissue for five representative CL species, compared to another representative lipid species, to show increase in relative abundance of CLs associated with FAIMS selective imaging. Scale bar= 3mm

Table S2. Representative ganglioside species detected during DESI-MSI and FAIMS-DESI-MSI analysis of rat brain tissue and identified using high mass accuracy and tandem MS analyses.[a]

Measured *m/z*	Tentative Attribution[b]	Mass Error (ppm)[c]	Proposed Formula

917.4798	GD1 d36:2 $[M-2H]^{2-}$	-1.09	$C_{84}H_{148}N_4O_{39}$
918.4832	GD1 d36:1 $[M-2H]^{2-}$	3.70	$C_{84}H_{150}N_4O_{39}$
919.4886	GD1 d36:1 $[M-2H]^{2-}$	6.31	$C_{84}H_{152}N_4O_{39}$
931.4957	GD1 d38:1 $[M-2H]^{2-}$	-1.40	$C_{86}H_{152}N_4O_{39}$
932.4993	GD1 d38:0 $[M-2H]^{2-}$	3.11	$C_{86}H_{154}N_4O_{39}$
952.5009	Acetylated GD1b d38:1 $[M-2H]^{2-}$	-1.26	$C_{88}H_{154}N_4O_{40}$
1063.0278	GT1 d36:1 $[M-2H]^{2-}$	-1.22	$C_{95}H_{167}N_5O_{47}$
1064.0313	GT1 d36:0 $[M-2H]^{2-}$	2.82	$C_{95}H_{167}N_5O_{47}$
1073.0093	GT1 d38:4 $[M-2H]^{2-}$	1.40	$C_{97}H_{161}N_5O_{47}$
1074.0175	GT1 d38:3 $[M-2H]^{2-}$	1.02	$C_{97}H_{163}N_5O_{47}$
1075.0205	GT1 d38:2 $[M-2H]^{2-}$	5.58	$C_{97}H_{165}N_5O_{47}$
1077.0433	GT1 d38:1 $[M-2H]^{2-}$	-1.11	$C_{97}H_{169}N_5O_{47}$
1078.0454	GT1 d38:0 $[M-2H]^{2-}$	4.17	$C_{97}H_{171}N_5O_{47}$
1082.0055	GT1 d36:1- Potassium adduct $[M-3H+K]^{2-}$	-1.02	$C_{95}H_{165}N_5O_{47}$
1083.0168	GT1 d36:0- Potassium adduct $[M-3H+K]^{2-}$	-4.25	$C_{95}H_{167}N_5O_{47}$
1084.0323	Acetylated GT1 d36:1 $[M-2H]^{2-}$	-0.55	$C_{97}H_{165}N_5O_{48}$
1085.0360	Acetylated GT1 d36:0 $[M-2H]^{2-}$	3.32	$C_{97}H_{167}N_5O_{48}$
1096.0210	GT1 d38:1- Potassium adduct $[M-3H+K]^{2-}$	-0.82	$C_{97}H_{169}N_5O_{47}$
1097.0294	GT1 d38:0- Potassium adduct $[M-3H+K]^{2-}$	-1.37	$C_{97}H_{171}N_5O_{47}$
1098.0490	Acetylated GT1 d38:1 $[M-2H]^{2-}$	-1.46	$C_{99}H_{169}N_5O_{48}$
1099.0496	Acetylated GT1 d38:0 $[M-2H]^{2-}$	5.10	$C_{99}H_{171}N_5O_{48}$

[a] Red text denotes species that were only detectable with the addition of FAIMS with DESI-MSI

[b] (X:Y) denotes the total number of carbons and doubles bonds within the steric acid and sphingosine chains

[c] Calculated based on the exact monoisotopic *m/z* of the deprotonated molecular ion.

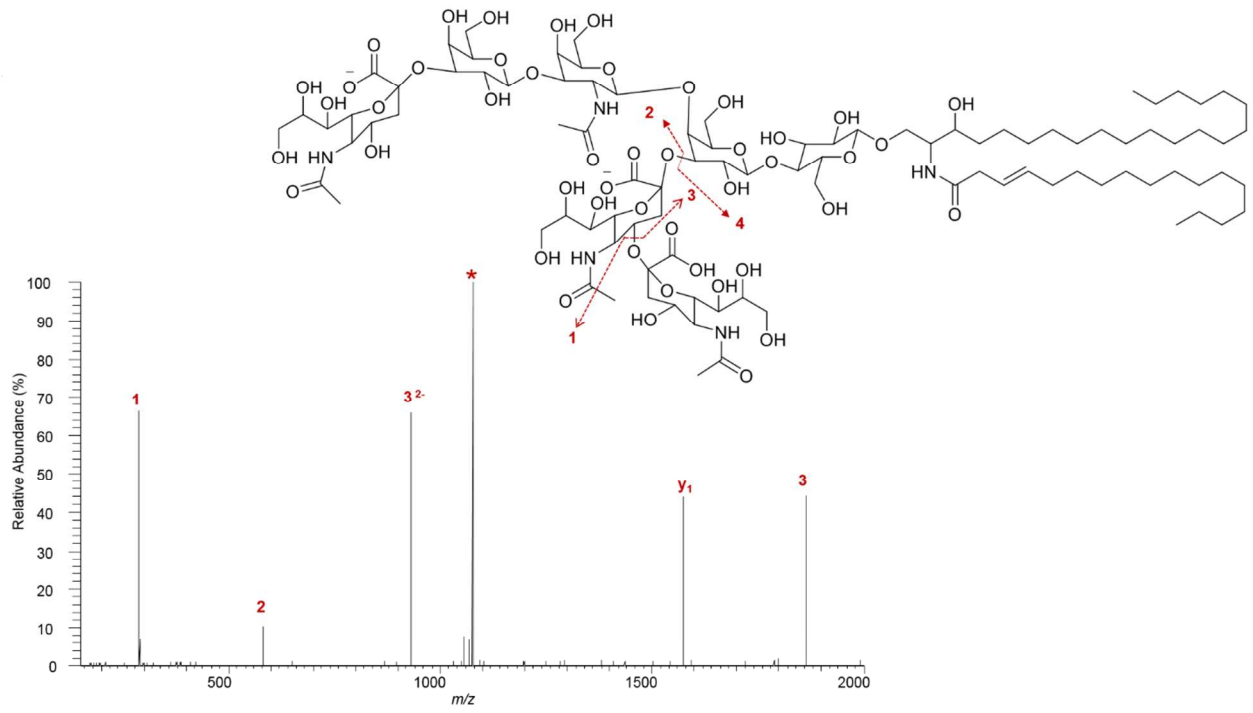

Figure S5. MSMS of *m/z* 1077.043, identified at GT1 d38:1 ganglioside

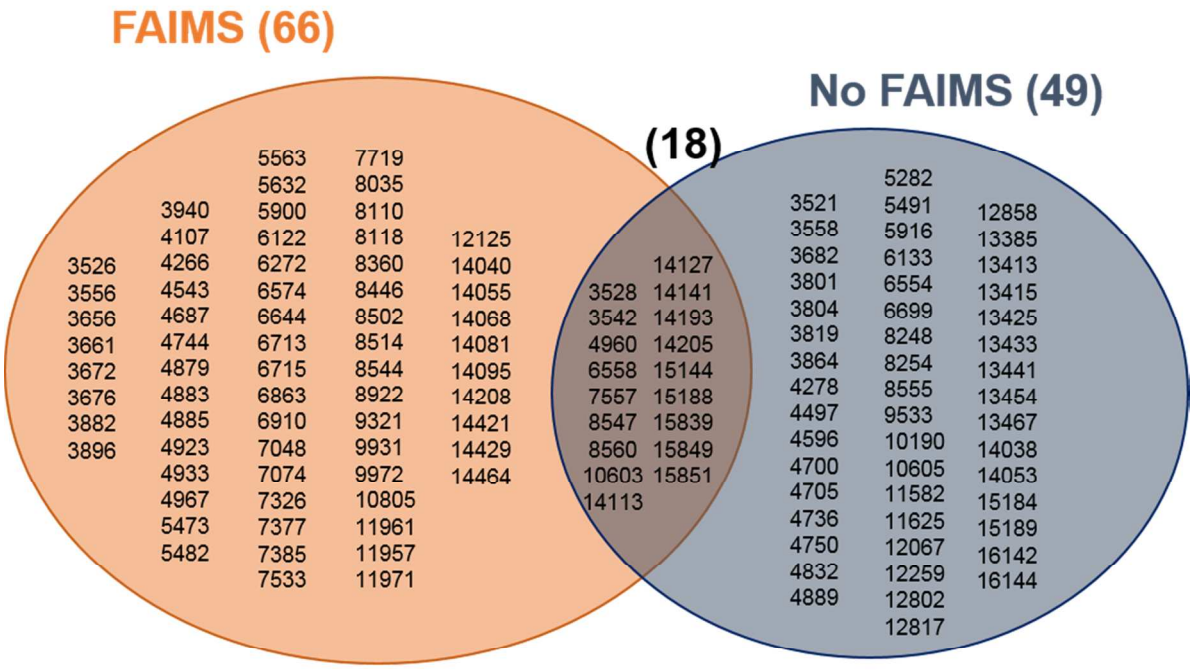

Figure S6. Molecular weights of all protein, proteoforms and protein fragment species detected during LMJ-SSP-MS and LMJ-SSP-FAIMS-MS profiling experiments of a rat brain tissue sections.

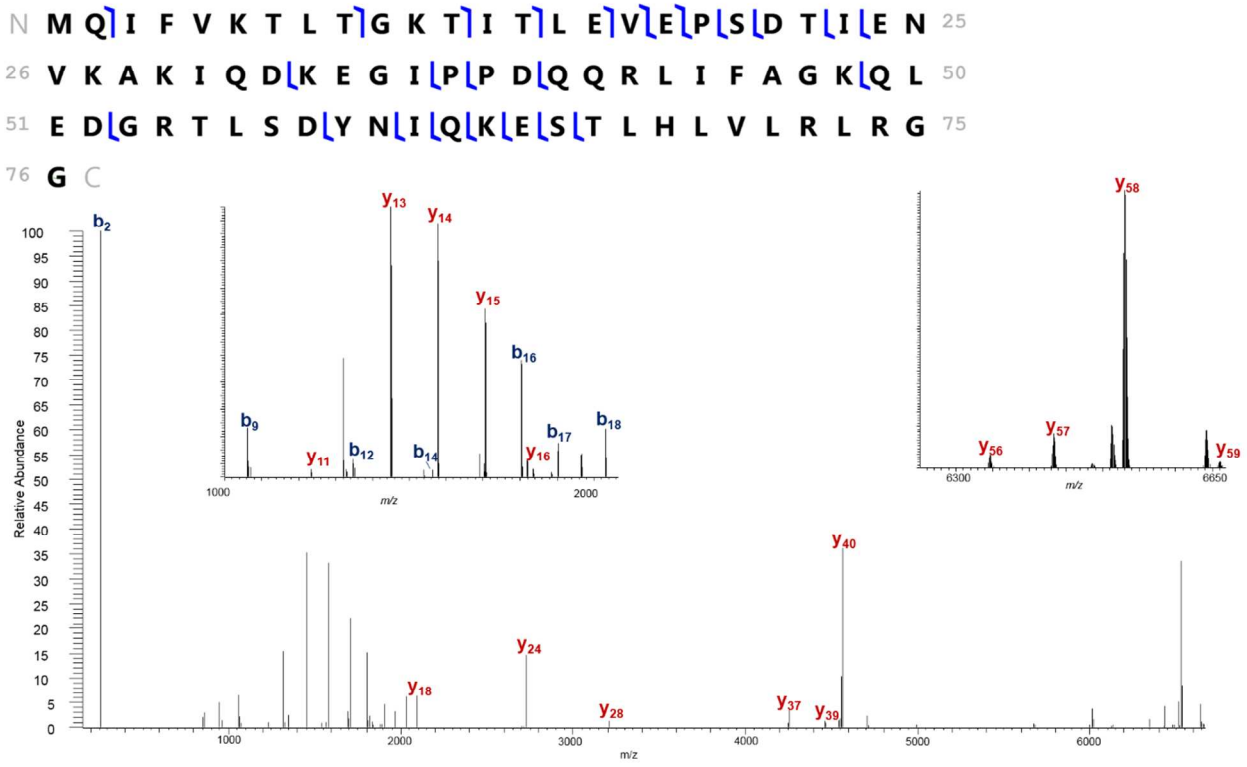

PCS	560.77
P-Score	4.1E-51
Fragments Explained	51%
Residue Cleavages	32%

Figure S7. MS/MS of ion cluster at *m/z* 857.46 from a rat brain tissue section, identified at ubiquitin. The sequence coverage map of the fragments compared to the sequence of rat ubiquitin is shown, as well as the ProSight Lite scores.

Table S3. Matching fragment ions identified from MS/MS of ion *m/z* 857.46 compared with the sequence of rat ubiquitin.

Name	Ion Type	Theoretical Mass[a]	Observed Mass[a]	Mass Difference (Da)	Mass Difference (ppm)
B2	B	259.09907	259.097903	-0.001167	-4.504068656
B9	B	1061.59433	1061.589782	-0.004548	-4.284122354
B12	B	1347.75843	1347.752456	-0.005974	-4.432545081
B14	B	1561.89017	1561.889998	-0.000172	-0.11012298
B16	B	1804.01682	1804.010171	-0.006649	-3.685664083
B17	B	1903.08523	1903.079469	-0.005761	-3.027189696
B18	B	2032.12782	2032.118804	-0.009016	-4.436728788
Y11	Y	1233.766945	1233.761436	-0.005509	-4.465186899
Y12	Y	1320.798975	1320.79362	-0.005355	-4.05436414
Y13	Y	1449.841565	1449.836181	-0.005384	-3.713509207
Y14	Y	1577.936525	1577.930363	-0.006162	-3.905100048
Y15	Y	1705.995105	1705.988989	-0.006116	-3.585004425
Y16	Y	1819.079165	1819.072672	-0.006493	-3.569388361
Y18	Y	2096.185425	2096.176443	-0.008982	-4.284926273
Y24	Y	2725.498705	2725.485762	-0.012943	-4.748855678
Y28	Y	3210.710875	3210.694521	-0.016354	-5.093576045
Y37	Y	4252.319205	4252.300703	-0.018502	-4.351037424
Y39	Y	4464.398905	4464.380932	-0.017973	-4.025849926
Y40	Y	4561.451665	4561.434382	-0.017283	-3.788925384
Y44	Y	4988.694735	4988.676274	-0.018461	-3.700567178
Y53	Y	6014.245275	6014.226124	-0.019151	-3.184273192
Y54	Y	6127.329335	6127.303402	-0.025933	-4.232349623
Y56	Y	6343.403955	6343.374982	-0.028973	-4.567421562
Y57	Y	6430.435985	6430.386656	-0.049329	-7.671175036
Y58	Y	6527.488745	6527.470469	-0.018276	-2.79985163
Y59	Y	6656.531335	6656.502773	-0.028562	-4.290823338

[a] Calculated based on monoisotopic masses

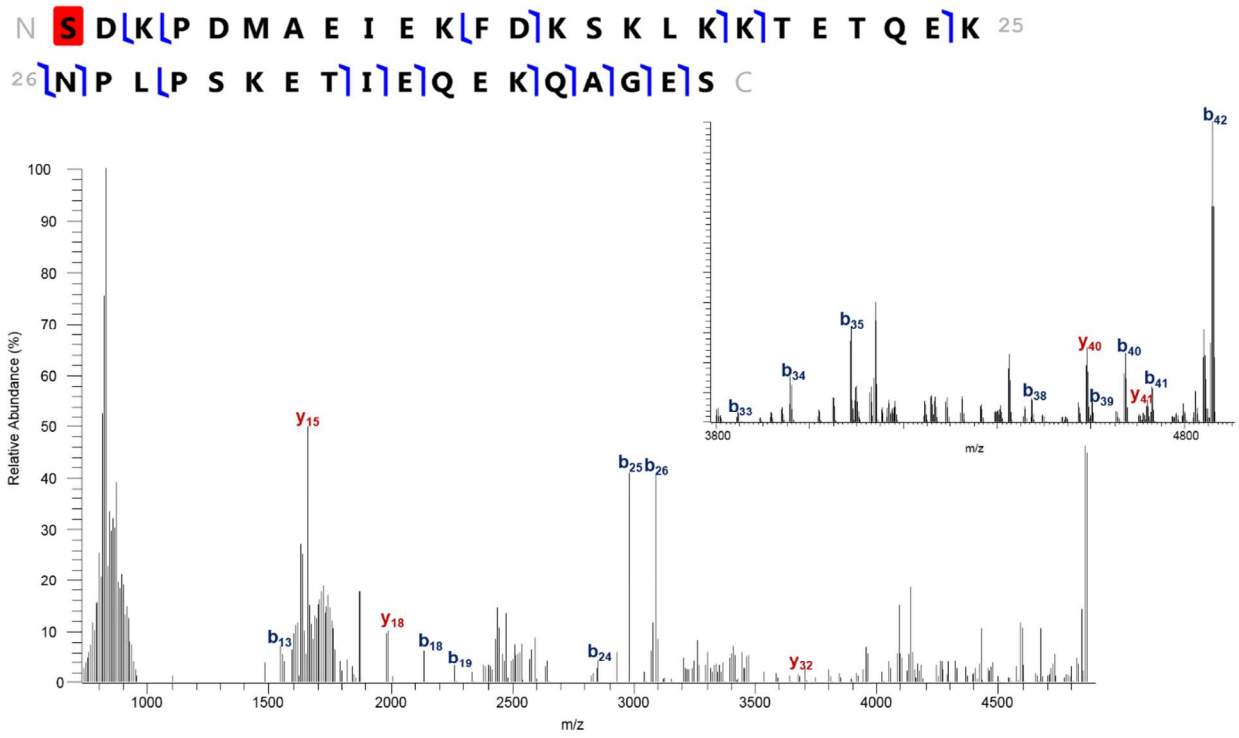

PCS	**110.46**
P-score	**8.6E-15**
Fragments Explained	**2%**
Residue Cleavages	**43%**

Figure S8. MS/MS of ion cluster at *m/z* 828.06 from a rat brain tissue section, identified as thymosin β-4. The sequence coverage map of the fragments compared to the sequence of rat thymosin β-4 is shown, as well as the ProSight Lite scores. The red highlight indicates an acylation.

Table S4. Matching fragment ions identified from MS/MS of ion *m/z* 828.09 compared with the sequence of rat thymosin β-4.

Name	Ion Type	Theoretical Mass[a]	Observed Mass[a]	Mass Difference (Da)	Mass Difference (ppm)
B13	B	1547.681345	1547.679601	-0.001744467	-1.127148612
B18	B	2132.082315	2132.07922	-0.003095467	-1.451851487
B19	B	2260.177275	2260.172114	-0.005161467	-2.283655772
B24	B	2848.416395	2848.414334	-0.002061467	-0.72372385
B25	B	2976.511355	2976.507654	-0.003701467	-1.243558797
B26	B	3090.554285	3090.550168	-0.004117467	-1.332274569
B33	B	3842.961125	3842.952632	-0.008493467	-2.210136039
B34	B	3956.045185	3956.039649	-0.005536467	-1.39949536
B35	B	4085.087775	4085.072164	-0.015611467	-3.821574404
B38	B	4470.283905	4470.275728	-0.008177467	-1.82929475
B39	B	4598.342485	4598.337145	-0.005340467	-1.161389544
B40	B	4669.379595	4669.369511	-0.010084467	-2.159701664
B41	B	4726.401055	4726.387793	-0.013262467	-2.806039252
B42	B	4855.443645	4855.440068	-0.003577467	-0.736795058
Y15	Y	1659.795135	1659.792623	-0.002512467	-1.513721077
Y18	Y	1983.974885	1983.973092	-0.001793467	-0.903976604
Y32	Y	3674.900245	3674.894573	-0.005672467	-1.543570302
Y40	Y	4588.321745	4588.314041	-0.007704467	-1.679147041
Y41	Y	4716.416705	4716.410236	-0.006469467	-1.371691113

[a] Calculated based on monoisotopic masses

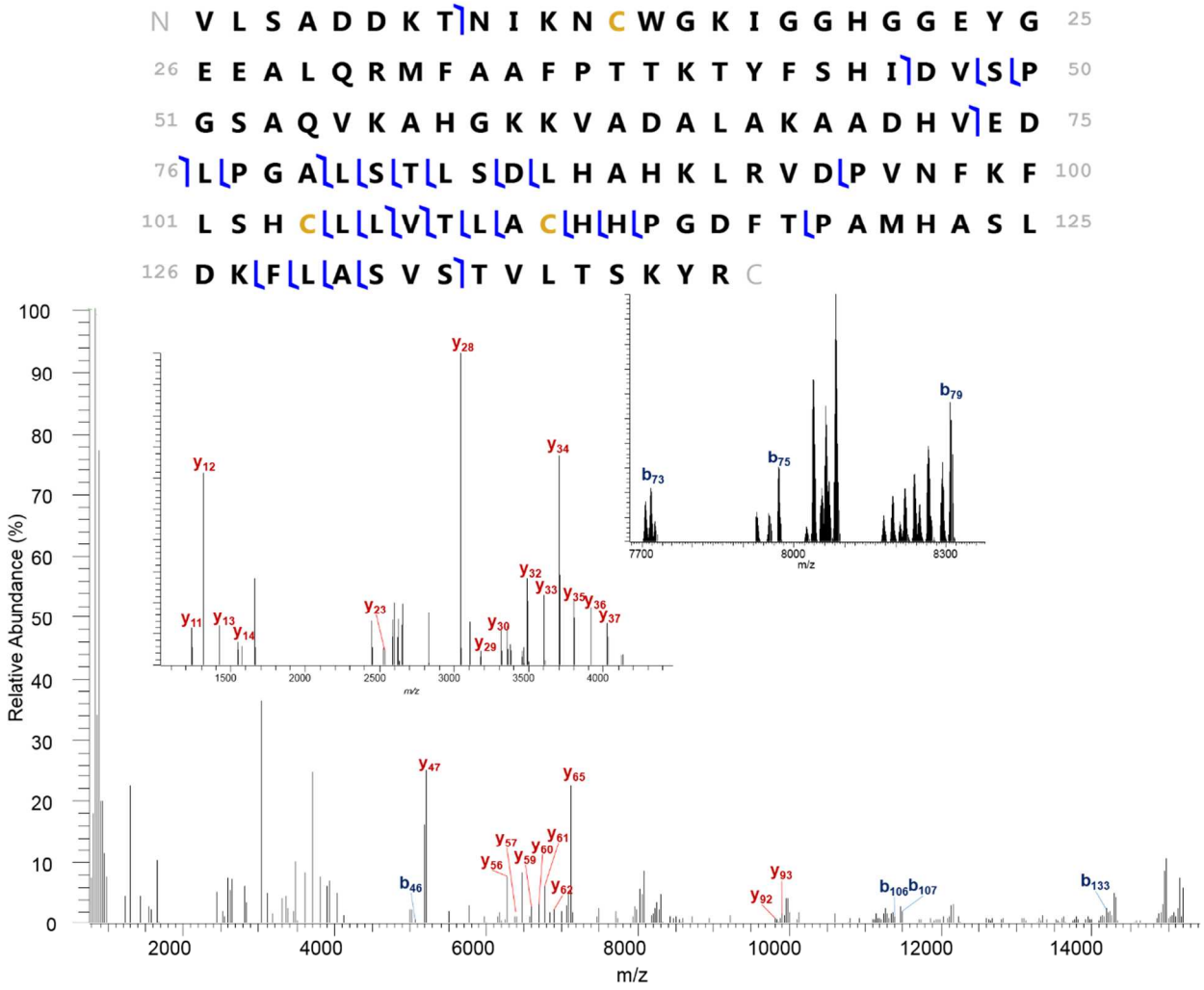

PCS	**157.05**
P-score	**8.2E-19**
Fragments Explained	**5%**
Residue Cleavages	**21%**

Figure S9. MS/MS of ion cluster at *m/z* 845.27 from a rat brain tissue section, identified as hemoglobin-α subunit. The sequence coverage map of the fragments compared to the sequence of rat hemoglobin-α subunit is shown, as well as the ProSight Lite scores.

Table S5. Matching fragment ions identified from MS/MS of ion *m/z* 845.27 compared with the sequence of rat hemoglobin-α subunit.

Name	Ion Type	Theoretical Mass[a]	Observed Mass[a]	Mass Difference (Da)	Mass Difference (ppm)
B8	B	829.41813	829.4205045	0.002374533	2.862890301
B46	B	5069.45919	5069.449327	-0.009863467	-1.94566452
B73	B	7720.87346	7720.873401	-5.94669E-05	-0.007702092
B75	B	7964.94299	7964.929299	-0.013691467	-1.718966087
B79	B	8303.13838	8303.122831	-0.015549467	-1.872721635
B106	B	11387.80784	11387.73042	-0.077416467	-6.798188726
B106	B	11387.80784	11387.78836	-0.019476467	-1.710291142
B107	B	11486.87625	11486.82282	-0.053426467	-4.651087529
B107	B	11486.87625	11486.84714	-0.029106467	-2.533888782
B133	B	14221.17578	14221.08355	-0.092226467	-6.485150616
Y11	Y	1239.682295	1239.680049	-0.002246467	-1.812131132
Y12	Y	1310.719405	1310.717153	-0.002252467	-1.71849663
Y13	Y	1423.803465	1423.801175	-0.002290467	-1.608695959
Y14	Y	1570.871875	1570.870583	-0.001292467	-0.8227704
Y23	Y	2521.336245	2521.331408	-0.004837467	-1.918612359
Y28	Y	3038.553495	3038.549185	-0.004310467	-1.418591737
Y29	Y	3175.612405	3175.606175	-0.006230467	-1.961973341
Y30	Y	3312.671315	3312.66361	-0.007705467	-2.326058383
Y32	Y	3486.717615	3486.712839	-0.004776467	-1.369903562
Y33	Y	3599.801675	3599.801924	0.000248533	0.069040781
Y34	Y	3700.849355	3700.844318	-0.005037467	-1.361165073
Y35	Y	3799.917765	3799.915976	-0.001789467	-0.470922528
Y36	Y	3913.001825	3912.995826	-0.005999467	-1.533213413
Y37	Y	4026.085885	4026.080364	-0.005521467	-1.371423025
Y47	Y	5198.665955	5198.648144	-0.017811467	-3.426161064
Y56	Y	6268.280425	6268.262426	-0.017999467	-2.871515896
Y57	Y	6383.307365	6383.292922	-0.014443467	-2.262693312
Y59	Y	6583.423455	6583.364484	-0.058971467	-8.957568548
Y59	Y	6583.423455	6583.367324	-0.056131467	-8.526182049
Y60	Y	6684.471135	6684.446011	-0.025124467	-3.758631965
Y61	Y	6771.503165	6771.466867	-0.036298467	-5.360474033
Y62	Y	6884.587225	6884.570863	-0.016362467	-2.376680888
Y65	Y	7109.698555	7109.6811	-0.017455467	-2.455162725
Y92	Y	9817.139035	9817.106118	-0.032917467	-3.353061087
Y93	Y	9904.171065	9904.124558	-0.046507467	-4.695745517

[a] Calculated based on monoisotopic masses

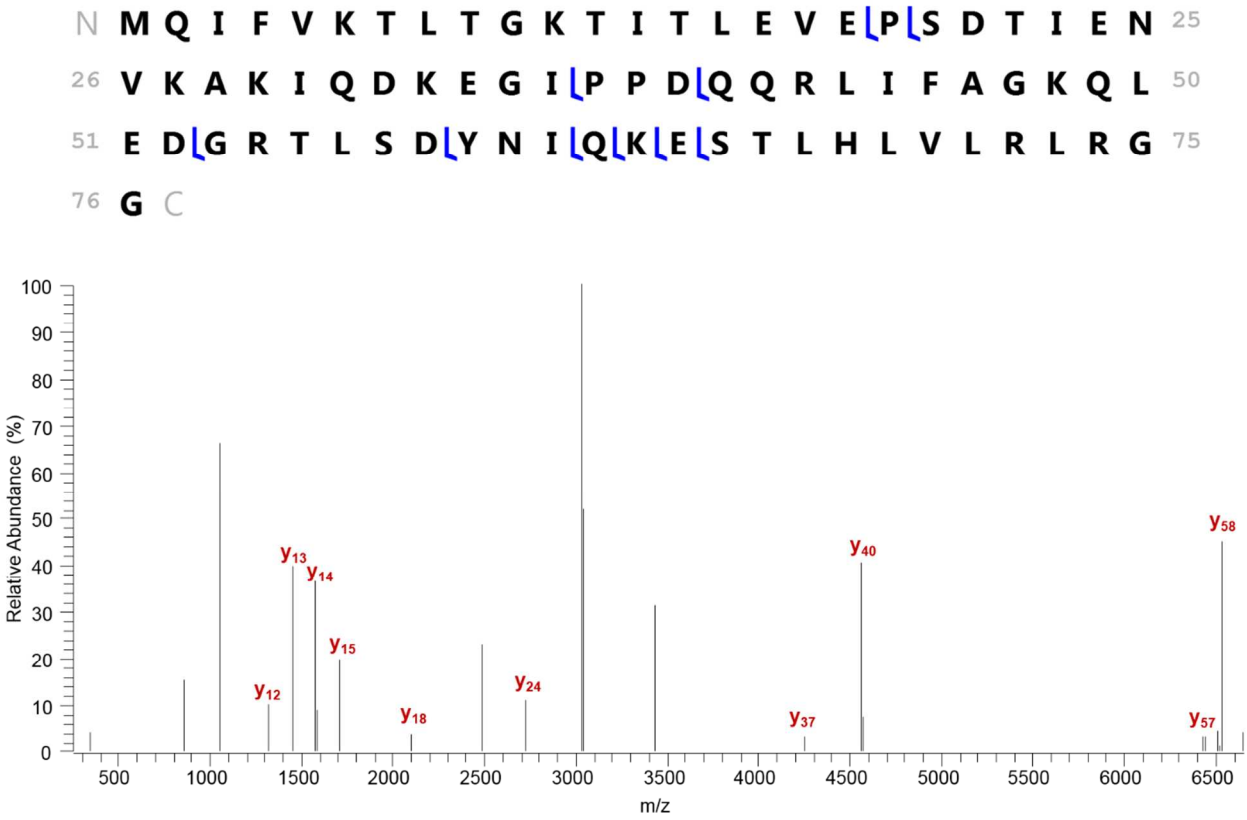

PCS	177.18
P-score	1.6E-20
Fragments Explained	50%
Residue Cleavages	13%

Figure S10. MS/MS of ion cluster at *m/z* 857. from an ovarian tumor tissue section, identified at ubiquitin. The sequence coverage map of the fragments compared to the sequence of human ubiquitin is shown, as well as the ProSight Lite scores.

Table S6. Matching fragment ions identified from MS/MS of ion *m/z* 952.52 compared with the sequence of rat ubiquitin.

Name	Ion Type	Theoretical Mass	Observed Mass	Mass Difference (Da)	Mass Difference (ppm)
Y12	Y	1320.798975	1320.79438	-0.004595	-3.47895485
Y13	Y	1449.841565	1449.837092	-0.004473	-3.085164688
Y14	Y	1577.936525	1577.931441	-0.005084	-3.221929348
Y15	Y	1705.995105	1705.989462	-0.005643	-3.307746888
Y18	Y	2096.185425	2096.178877	-0.006548	-3.123769454
Y24	Y	2725.498705	2725.489674	-0.009031	-3.31352203
Y37	Y	4252.319205	4252.303738	-0.015467	-3.637309255
Y40	Y	4561.451665	4561.431493	-0.020172	-4.422276389
Y57	Y	6430.435985	6430.416252	-0.019733	-3.068687729
Y58	Y	6527.488745	6527.462698	-0.026047	-3.990355406

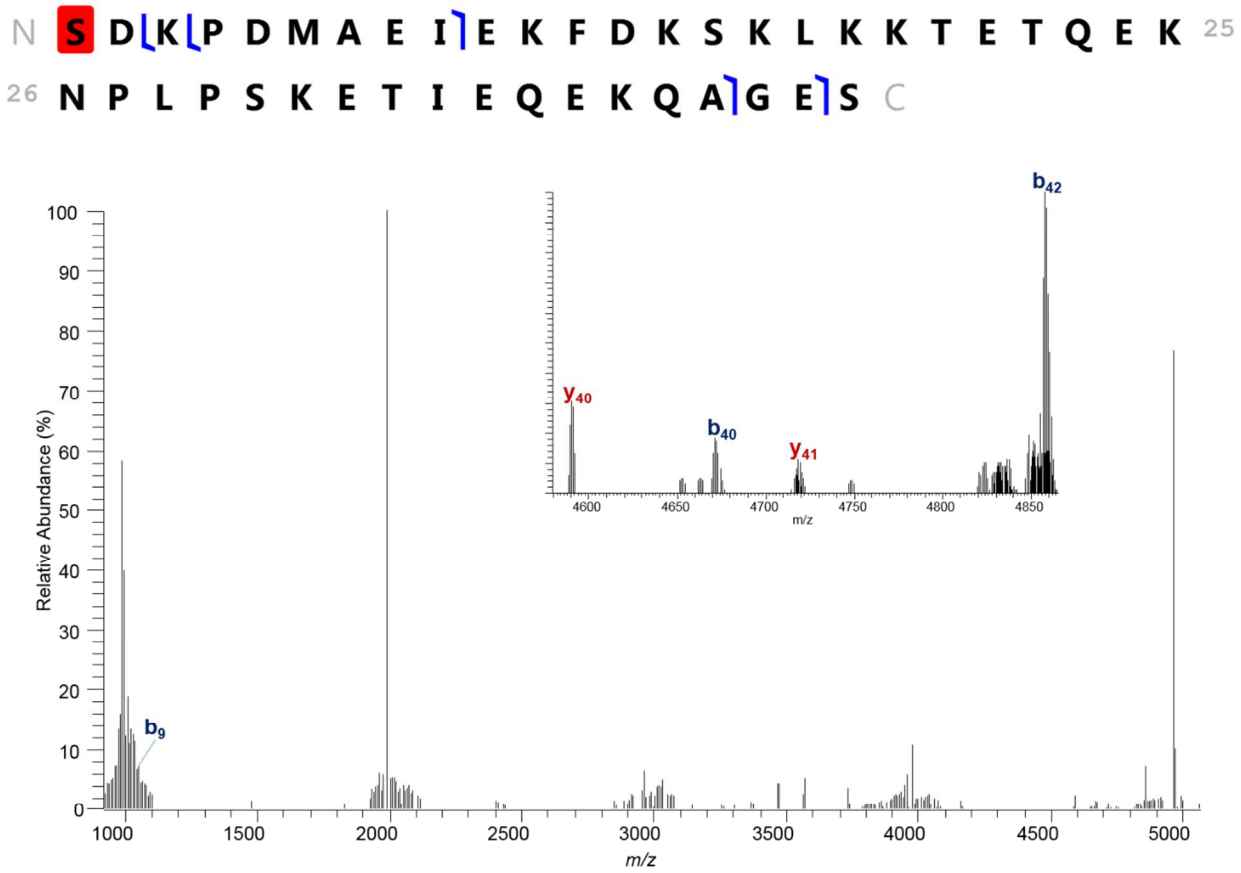

PCS	0.20
P-score	0.054
Fragments Explained	0%
Residue Cleavages	12%

Figure S11. MS/MS of ion cluster at *m/z* 933.50 from an ovarian tumor tissue section, identified as thymosin β-4. The sequence coverage map of the fragments compared to the sequence of human thymosin β-4 is shown, as well as the ProSight Lite scores. The red highlight indicates an acylation.

Table S7. Matching fragment ions identified from MS/MS of ion *m/z* 933.50 compared with the sequence of human thymosin β-4.

Name	Ion Type	Theoretical Mass[a]	Observed Mass[a]	Mass Difference (Da)	Mass Difference (ppm)
B9	B	1028.448445	1028.441021	-0.007424	-7.218640892
B40	B	4669.379595	4669.360756	-0.018839	-4.0345831
B42	B	4855.443645	4855.437948	-0.005697	-1.173322237
Y40	Y	4588.321745	4588.314136	-0.007609	-1.658340549
Y41	Y	4716.416705	4716.418703	0.001998	0.423626691

[a] Calculated based on monoisotopic masses

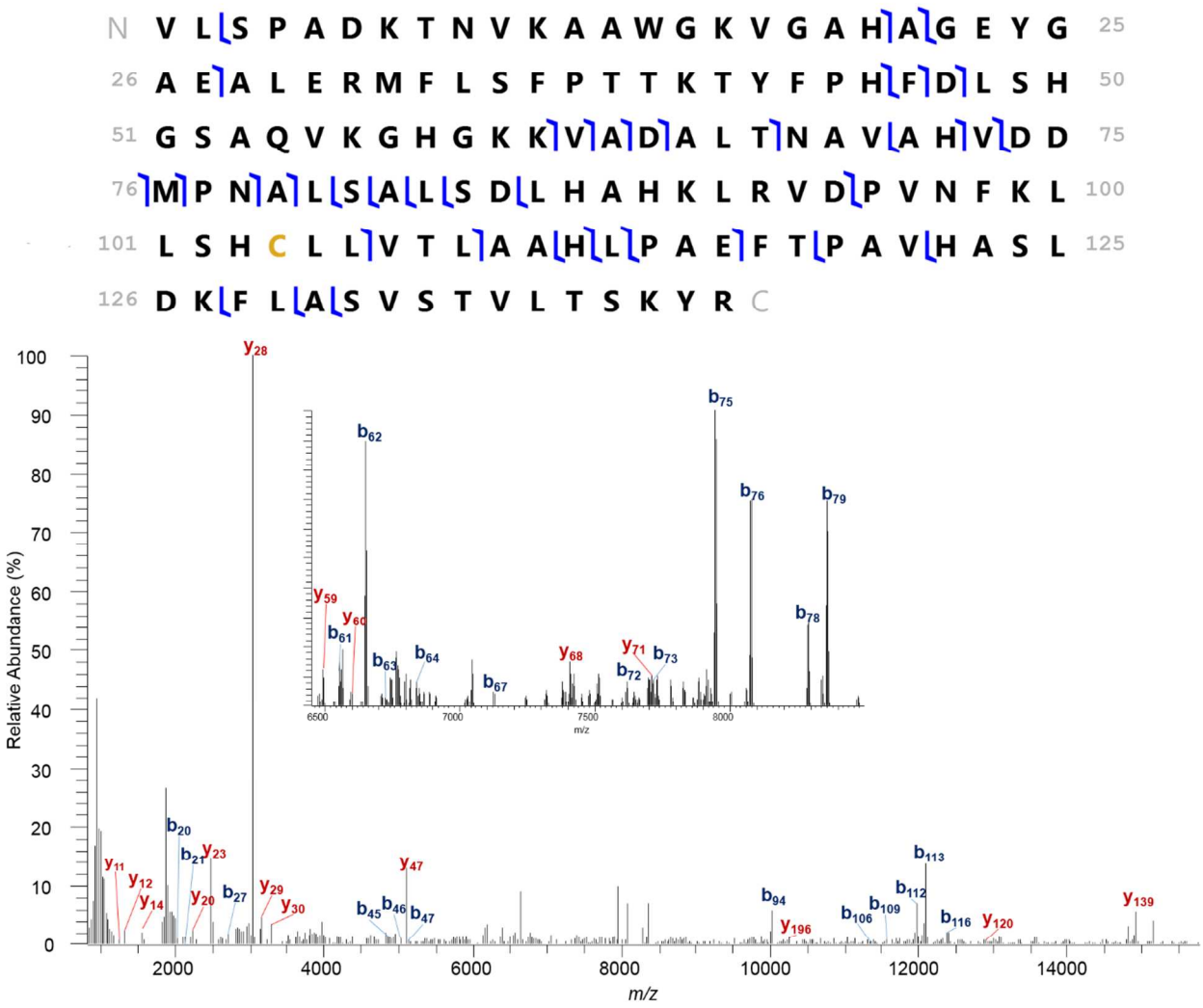

PCS	57.39
P-score	6.5E-10
Fragments Explained	2%
Residue Cleavages	26%

Figure S12. MS/MS of ion cluster at *m/z* 946.31 from a rat brain tissue section, identified as hemoglobin-α subunit. The sequence coverage map of the fragments compared to the sequence of rat hemoglobin-α subunit is shown, as well as the ProSight Lite scores.

Table S8. Matching fragment ions identified from MS/MS of ion *m/z* 946.31 compared with the sequence of human hemoglobin-α subunit.

Name	Ion Type	Theoretical Mass	Observed Mass	Mass Difference (Da)	Mass Difference (ppm)
B20	B	2030.10609	2030.103522	-0.002568	-1.264958522
B21	B	2101.1432	2101.140376	-0.002824	-1.34403024
B27	B	2707.37174	2707.364201	-0.007539	-2.784619448
B45	B	4874.46418	4874.459487	-0.004693	-0.962772487
B46	B	5021.53259	5021.527972	-0.004618	-0.919639556
B47	B	5136.55953	5136.554839	-0.004691	-0.913257205
B61	B	6551.33883	6551.353551	0.014721	2.247021621
B62	B	6650.40724	6650.399928	-0.007312	-1.099481541
B63	B	6721.44435	6721.432335	-0.012015	-1.787562222
B64	B	6836.47129	6836.453683	-0.017607	-2.575451465
B67	B	7121.64014	7121.596828	-0.043312	-6.081745096
B72	B	7613.88461	7613.866762	-0.017848	-2.344138494
B73	B	7712.95302	7712.936887	-0.016133	-2.091676166
B75	B	7943.0069	7942.996125	-0.010775	-1.356539171
B76	B	8074.04739	8074.031671	-0.015719	-1.946855058
B78	B	8285.14308	8285.151632	0.008552	1.03220909
B79	B	8356.18019	8356.159511	-0.020679	-2.474695319
B94	B	10012.09089	10012.08605	-0.00484	-0.483415507
B106	B	11376.85473	11376.81886	-0.03587	-3.152892503
B109	B	11690.05488	11690.02276	-0.03212	-2.747634662
B112	B	11969.18801	11969.16292	-0.02509	-2.096215714
B113	B	12082.27207	12082.26339	-0.00868	-0.718407923
B116	B	12379.40453	12379.45182	0.04729	3.820054503
Y11	Y	1239.682295	1239.681151	-0.001144	-0.922817084
Y12	Y	1310.719405	1310.717846	-0.001559	-1.189423148
Y14	Y	1570.871875	1570.868778	-0.003097	-1.971516614
Y20	Y	2222.205885	2222.209615	0.00373	1.67851234
Y23	Y	2489.364165	2489.361543	-0.002622	-1.053281009
Y28	Y	3034.612715	3034.60955	-0.003165	-1.042966697
Y29	Y	3147.696775	3147.698958	0.002183	0.693522965
Y30	Y	3284.755685	3284.749742	-0.005943	-1.809266981
Y47	Y	5104.793895	5104.791325	-0.00257	-0.503448338
Y56	Y	6174.408365	6174.404271	-0.004094	-0.66305948
Y58	Y	6376.467335	6376.464121	-0.003214	-0.504040848
Y59	Y	6489.551395	6489.560332	0.008937	1.377136793
Y60	Y	6560.588505	6560.59289	0.004385	0.66838516
Y61	Y	6647.620535	6647.615883	-0.004652	-0.699799271

Y68	Y	7403.931765	7403.925961	-0.005804	-0.783907819
Y71	Y	7711.096195	7711.105709	0.009514	1.233806421
Y96	Y	10242.42061	10242.41377	-0.006835	-0.667322722
Y120	Y	13015.74159	13015.74472	0.003135	0.240862189
Y139	Y	14904.73232	14904.73395	0.001635	0.109696704

[a] Calculated based on monoisotopic masses

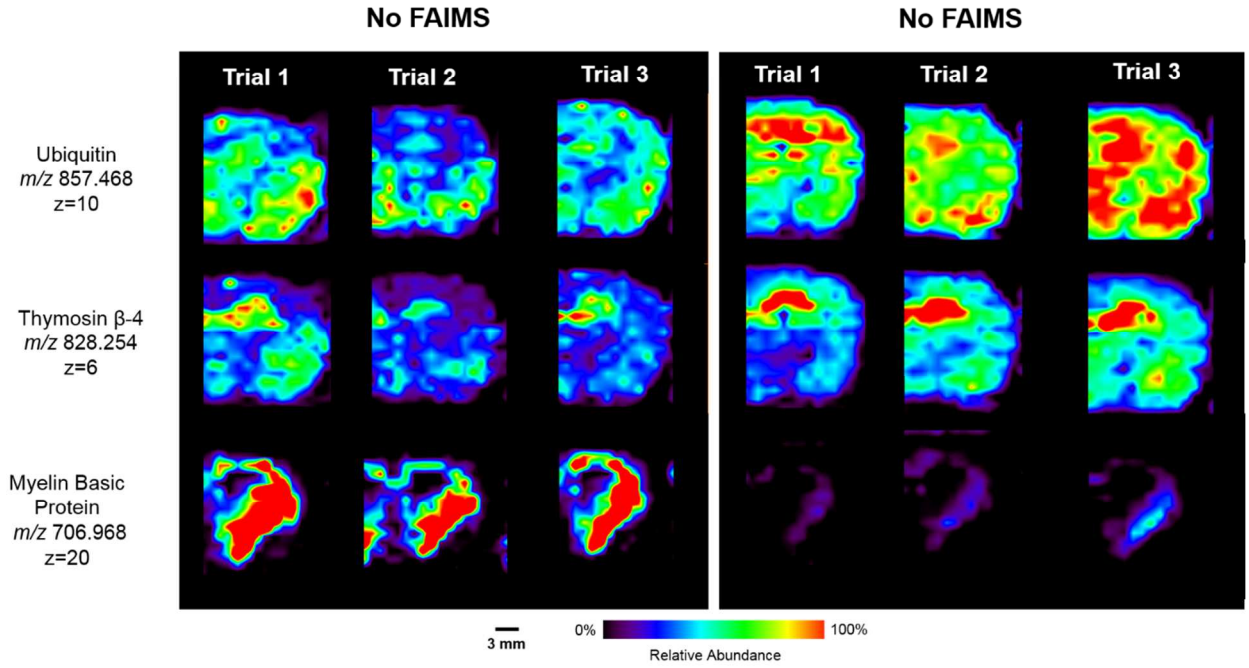

Figure S13. Ion images of three representative proteins on replicates (n=3) of serial sections of rat brain tissue half sections to show consistency of ion distribution when using LMJ-SSP and LMJ-SSP-FAIMS.

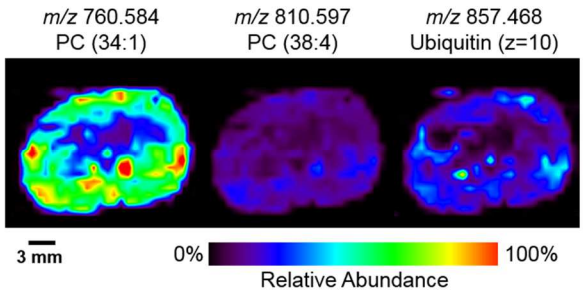

Figure S14. LMJ-SSP-FAIMS-MS lipid and protein ion images obtained through selective imaging for proteins.

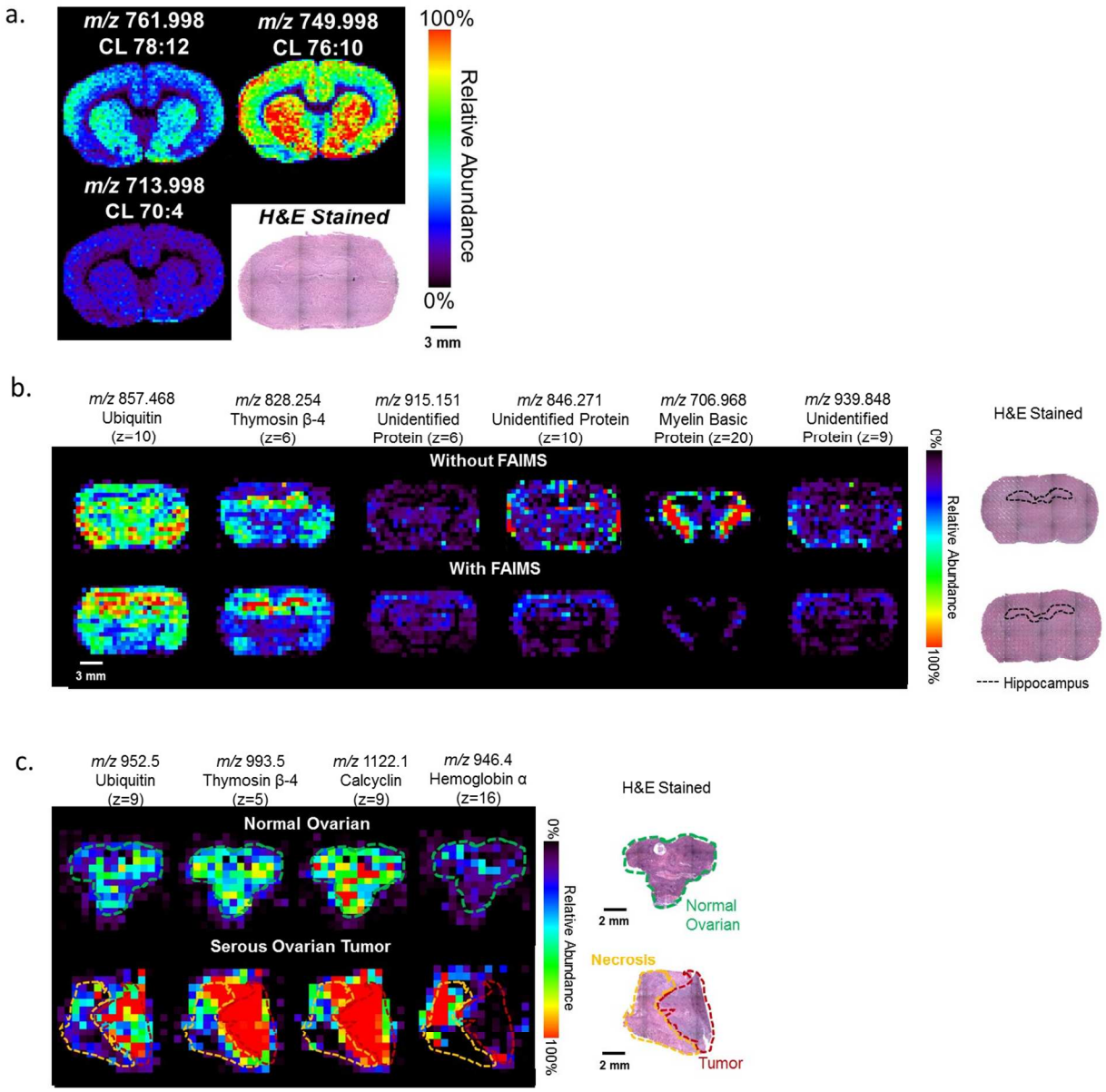

Figure S15. Voxel version of ion images displayed in a) Figure 2 (DESI-FAIMS ion images for selected CL species); b) Figure 4 (LMJ-SSP-MS and LMJ-SSP-FAIMS-MS ion images of rat brain tissue for six representative protein species including ubiquitin, thymosin β-4, MBP, and three unidentified proteins); and C) Figure 5 (LMJ-SSP-FAIMS-MS ion images of ubiquitin, thymosin β-4, calcyclin, and hemoglobin α-subunit for a normal ovarian tissue sample compared with the high grade serous ovarian tumor sample, containing both necrotic and tumor regions).